Express Polymer Letters Vol.17, No.10 (2023) 1031–1041
Available online at www.expresspolymlett.com
https://doi.org/10.3144/expresspolymlett.2023.77

Research article

The polymorphic composition of long-chain branched polypropylene processed by injection and compression molding

Lenka Gajzlerova, Jana Navratilova, Martina Polaskova, Lubomir Benicek, Roman Cermak*

Tomas Bata University in Zlin, Faculty of Technology, Vavreckova 5669, 760 01 Zlin, Czech Republic

Received 22 March 2023; accepted in revised form 7 July 2023

Abstract. The impact of injection molding processing parameters, including mold temperature, injection speed, and holding pressure, on the supermolecular structure of long-chain branched polypropylene (LCB-PP) was investigated. Commercial LCB-PP was processed under different conditions, with four sets of processing parameters applied. Holding pressure was varied from 30–70 MPa by 10 MPa in the P-SET, mold temperature was raised from 40 to 120 °C in 20 °C steps in the T-SET, and injection speed increased from 20 to 140 mm/s in 30 mm/s steps in S-SET1 and S-SET2, with mold temperatures at 40 or 120 °C. The polymorphic composition of the specimens was analyzed using wide-angle X-ray scattering, demonstrating a strong dependence on the processing parameters. The skin of the specimens showed an increase in β-phase content with higher mold temperature and injection speed. Conversely, growing holding pressure slightly suppressed β-phase content and promoted the formation of the γ-phase, which was predominantly manifested in the core of the specimens. The polymorphic composition, with both β- and γ-phases present in notable amounts, had a beneficial effect on the impact strength of the specimens.

Keywords: *processing technologies, material testing, mechanical properties, long-chain branched polypropylene, polymorphism*

1. Introduction

Polymorphism of polymers is a very interesting phenomenon predetermining the end-use properties of products. As a result, it is essential to carefully control specific nucleation and processing parameters to achieve the desired characteristics. Flow-induced crystallization is particularly important in manufacturing processes such as injection and blow molding [1–4]. The utilization of flow fields has been shown to accelerate crystallization kinetics [4], enhance nucleation density [5], and induce various morphologies, such as oriented crystalline structures like shish-kebab [6] or β-crystals [7]. Therefore, understanding the mechanisms of applied shear fields, as characterized by flow rate and temperature, and their impact on polymorphism is crucial in optimizing processing conditions.

Isotactic polypropylene (iPP) and its modifications, *e.g.*, long-chain branched polypropylene, are among the most widely used polymorphic polymers due to their versatility in terms of both property function and processability [8]. The molecular structure of iPP allows it to solidify into several crystallographic modifications, including the α-, β-, and γ-phases, as well as the mesomorphic 'smectic' phase formed during high undercooling. Only a small fraction of the

*Corresponding author, e-mail: j1navratilova@utb.cz

material, the ε-crystal modification, is obtained with the most stereodefective or 'an-isotactic' part of iPP produced with a zirconene catalyst [9, 10].

Nevertheless, only monoclinic α-phase and trigonal β-phase possess relevance to practice [8, 11]. The α-modification is the most common phase of iPP and grows dominantly under normal processing conditions. The β-modification is thermodynamically less favorable and recrystallizes into the α-phase on heating. However, several special crystallization techniques have been developed – the temperature gradient method [12], shear-induced crystallization [13, 14], or the most effective specific nucleation caused by an insertion of the heterogeneous β-nucleating agent [15–18]. Nucleating agents, which are typically low-molecular-mass organic or inorganic substances added to polymers, can induce specific β-nucleation that enhances the toughness of iPP while reducing its stiffness and heat resistance [18–20]. In comparison to the ordinary α-phase, this modification also improves resistance to photodegradation [21–23]. The orthorhombic γ-phase is another metastable polymorph of iPP that can form in the presence of chain irregularities, such as stereo- or regio-irregularities, through methods such as metallocene catalyzed crystallization [24, 25], high-pressure crystallization of homopolymers [26], crystallization of very low molecular weight fractions of iPP [27], or through the crystallization of propylene copolymers containing small amounts of 1-olefin co-units [28]. Long-chain branched polypropylene (LCB-PP) typically contains a higher content of chain irregularities, resulting in a higher tendency to form γ-phase. LCB-PP can be produced by introducing a long-chain branching architecture onto the polypropylene backbone using techniques such as in situ polymerization in a reactor [29], high energy irradiation [30], or melt-free radical grafting, with the latter being the most commonly used method [31, 32]. The crystalline system of LCB-PP usually consists of α- and γ-phases, with the formation of β-phase being suppressed under standard processing conditions [15, 33]. LCB-PP exhibits unique crystallization behavior compared to iPP, including higher crystallization temperature, faster overall crystallization, and a broader melting scale [15, 34]. LCB-PP also exhibits high melt strength and strain hardening in elongational flow, making it suitable for various industrial processes such as foaming, blow film processing, blow molding, and thermoforming [35, 36].

However, certain processing techniques that involve a dominant shear field, such as injection molding, can facilitate the development of desirable crystalline structures in long-chain branched polypropylene. Recent research by Zhou *et al*. [37] has revealed an increase in the β-phase content of LCB-PP with increasing LCB structure content, along with the occurrence of the trigonal modification. While flow-induced crystallization of isotactic polypropylene has been extensively studied, less is known about the crystallization behavior of LCB-PP under complex flow fields [1, 4, 37, 38]. Therefore, the objective of this study is to investigate the influence of important processing parameters, including injection speed, holding pressure, and mold temperature, on the morphology evolution and distribution of β- and/or γ-crystals in the 'skin-core' structure of LCB-PP. This structure results from non-homogeneous flow fields and thermo-mechanical conditions in the thickness direction, with the final polymorphic composition reflecting mechanical properties such as impact strength. The results of this research could offer a comprehensive understanding of shear-induced crystallization behavior in LCB-PP and potentially enable the prediction and customization of the final multi-component crystalline system, thereby enhancing the prospects for successful processing and industrial utilization.

2. Experimental

2.1. Material

In this study, Daploy WB140HMS was utilized, a commercially available long-chain branched polypropylene supplied by Borealis Company in Vienna, Austria. This propylene-based polymer is produced through in situ polymerization, where monomers are grafted onto isotactic polypropylene using peroxides to create long-chain branches. The examined material has a melt flow rate of 2.8 g/10 min, as measured at 230 °C and 2.16 kg using the ISO 1133 standard, weight-averaged molecular weight of 600 000, and polydispersity index of 5.2.

2.2. Specimens preparation

For the preparation of specimens, a Demag NC4 injection molding machine, Demag AG, Dusseldorf, Germany, was used to mold Charpy test specimens following ISO 179-1 with dimensions of 80×10×4 mm. The parameters of the mold were: sprue diameter ranging from 3.5 to 6.0 mm, runner

diameter of 10 mm, the gate located at the top side of the specimen with dimensions of 7×4 mm, and a length of 5 mm. Four sets of processing parameters were employed, namely P-SET with holding pressure varied from 30 to 70 MPa by 10 MPa, T-SET with mold temperature precisely controlled at temperatures increasing from 40 to 120 °C in 20 °C increments, and S-SET1 and S-SET2 with injection speed ranging from 20 to 140 mm/s in 30 mm/s increments and a mold temperature of 40 or 120 °C, respectively. Other parameters remained constant, as shown in Table 1. For the investigation of the effect of processing parameters on the supermolecular structure of the material, the same Charpy test specimens were also compression-molded (CM) in a manual press from Versta, Zlin, Czech Republic: at a pressing temperature of 210 °C for 5 min and cooled at 80 °C for 5 min. The skin and core of the specimens were analyzed using wide-angle X-ray scattering (WAXS), where the core was exposed by grinding off two millimeters of material from the surface using a Buehler Phoenix Alpha 1, Buehler, Lake Bluff, Illinois, USA. Grinding was carried out under running water at a temperature of 15 °C.

2.3. Wide-angle X-ray scattering

Wide-angle X-ray scattering was applied in order to obtain information about the crystallinity and polymorphic composition of specimens. X-ray patterns were taken of both the skin and the core of the specimens using an XRDynamic 500 diffractometer, Anton Paar, Graz, Austria, with Bragg-Brentano beam geometry in reflection mode, CuK_α radiation with a Ni filter ($\lambda = 0.154$ nm) and the diffraction angle interval of $2\theta = 5–30°$ was used. The peak search algorithm was based on the second derivative of the measured data, which showed local minima at peak positions. Peaks were searched and fitted using a variant of the pseudo-Voigt profile, which is a linear combination of a Gaussian and a Lorentzian curve. For the determination of the total crystallinity (X) of the specimens and polymorphic composition (K_β, K_γ), the data were fitted using a linear combination of Chebyshev polynomials. The total crystallinity was calculated from the share of the fitted areas of the crystalline part (A_C) and amorphous part (A_A) using Equation (1):

$$X = \frac{A_C}{A_C + A_A} \cdot 100\ [\%] \tag{1}$$

The multi-component α/β/γ crystalline system was determined using Equations (2)–(5) given by Obadal *et al*. [39] based on Turner-Jones *et al*.' work [40]. The K_β and K_γ, respectively, represent relative β- and γ-phase content in the three-phase crystalline system of polypropylene and can be calculated as Equation (2):

$$K_\beta = \frac{I_\beta}{I_{\alpha_1} + I_{\alpha_2} + I_{\alpha_3} + I_\beta + I_\gamma} \cdot 100\ [\%] \tag{2}$$

where $I_{\alpha 1}$, $I_{\alpha 2}$, $I_{\alpha 3}$, I_β, and I_γ denote the integral intensities of the individual diffraction peaks (α_1 at $2\theta = 14.20°$, α_2 at 17.00°, α_3 at 18.80°, β at 16.20° and γ at 20.05°).

The common content of both α- and γ-phases ($K_{\alpha+\gamma}$) in a three-phase crystalline system can be expressed (Equation (3)):

$$K_{\alpha+\gamma} = 1 - K_\beta \tag{3}$$

In the γ/α crystalline system, reflections at $2\theta = 14.2°$ and 17.0° are shared by both α- and γ-phases. Thus, γ-phase part (G) in the crystalline part can be derived only from the intensities of (130) α_3 reflection ($I_{\alpha 3}$ at 18.80°) and (117) γ reflection (I_γ at 20.05°), that are unique reflections for each phase [41] (Equations (4) and (5)):

$$G = \frac{I_\gamma}{I_{\alpha_3} + I_\gamma} \cdot 100\ [\%] \tag{4}$$

$$K_\gamma = G \cdot K_{\alpha+\gamma} \tag{5}$$

Table 1. Processing parameters of injection molding.

	Parameter	Unit	Value
	Temperatures of heating zones	°C	190; 220; 230
	Melt temperature (nozzle)	°C	240
	Holding pressure time	s	60
T-SET	Mold temperature	°C	40 / 60 / 80 / 100 / 120
	Injection speed	mm/s	80
	Holding pressure	MPa	50
P-SET	Holding pressure	MPa	30 / 40 / 50 / 60 / 70
	Mold temperature	°C	40
	Injection speed	mm/s	80
S-SET1	Injection speed	mm/s	20 / 50 / 80 / 110 / 140
	Mold temperature	°C	40
	Holding pressure	MPa	50
S-SET2	Injection speed	mm/s	20 / 50 / 80 / 110 / 140
	Mold temperature	°C	120
	Holding pressure	MPa	50

The above method allows for a relative calculation of the polymorphic composition in three-phase crystalline systems of polypropylene; however, the results can be used to quantify multiphase crystalline systems.

2.4. Charpy impact test

Non-instrumented Charpy impact tests were performed on a Charpy impact tester Impact 803, Tinius Olsen, Salfords Surrey, United Kingdom, using the specimens with a V-notch. The tests were carried out with a striker energy of 1.97 J and a span length of 62 mm at 23 °C. The average values of notched Charpy impact energy were obtained from each group of ten specimens.

3. Results and discussion

3.1. Polymorphic composition

The skin and core layers of the specimens prepared under various processing conditions were analyzed using X-ray diffractograms (Figures 1–5). The peaks of the main planes of various phases demonstrate common diffraction spectra of polymorphic crystalline systems. Injection-molded specimens show monoclinic α-phase α_1 (110), α_2 (040), and α_3 (130), trigonal β-phase (300), and orthorhombic γ-phase (117) peaks, as seen in Figures 1–4. The skin layer of all specimens exhibits a distinct β-diffraction peak, while the core layer shows a less significant peak. Diffractograms of compression-molded specimens (Figure 5) almost solely contain peaks corresponding to α-phase and γ-phase (117), with a negligible amount of trigonal β-phase. These results illustrate the significant influence of processing conditions on the LCB-PP's polymorphic composition.

Crystallinity and the relative amount of β-phase and γ-phase in the skin and core of specimens were determined by deconvoluting WAXS patterns and evaluated using Equations (1)–(5). These parameters, as a function of mold temperature, holding pressure, or injection speed, are shown in Figures 6–9. The reported dependences were determined at a significance level of $\alpha = 0.05$. It was found that the processing technology used significantly affects the crystallinity achieved. Table 2 shows that compression-molded specimens had lower crystallinity, reaching around 55% in the skin and 54% in the core, compared to injection-molded specimens. The content of γ-phase in compression-molded specimens was around 12%, regardless of the skin/core position

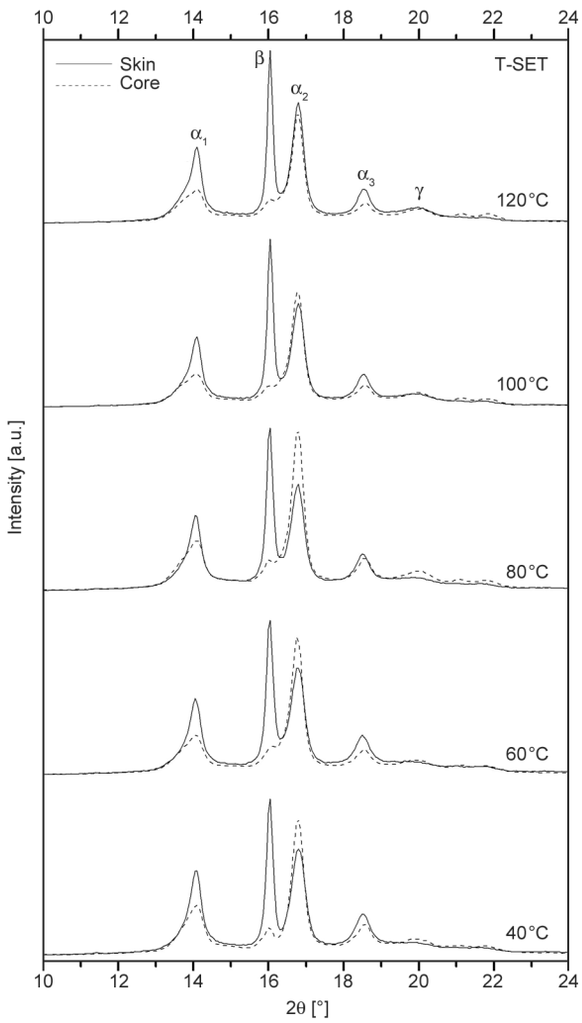

Figure 1. X-ray diffraction patterns of specimens injection-molded into the mold with various temperatures – T-SET.

(Figure 6), and the amount of β-phase was negligible. The effect of processing parameters on the crystallinity of injection-molded specimens was not significant (Table 2). The skin layer had crystallinity of around 69%, with the core having slightly lower values in most cases, regardless of holding pressure, injection speed, or mold temperature, except for high mold temperature (120 °C), which led to an increase in skin layer crystallinity. The skin crystallized at almost the same temperature as the mold temperature, while the core solidified under more complex thermal conditions due to the low thermal conductivity of polypropylene melt. There was no observable dependence of crystallinity on mold temperature in the core.

An interesting observation can be made by comparing the morphology evolution throughout the thickness of injection-molded specimens - the co-existence of α-, β-, and γ-phases. It has been reported that γ-crystals

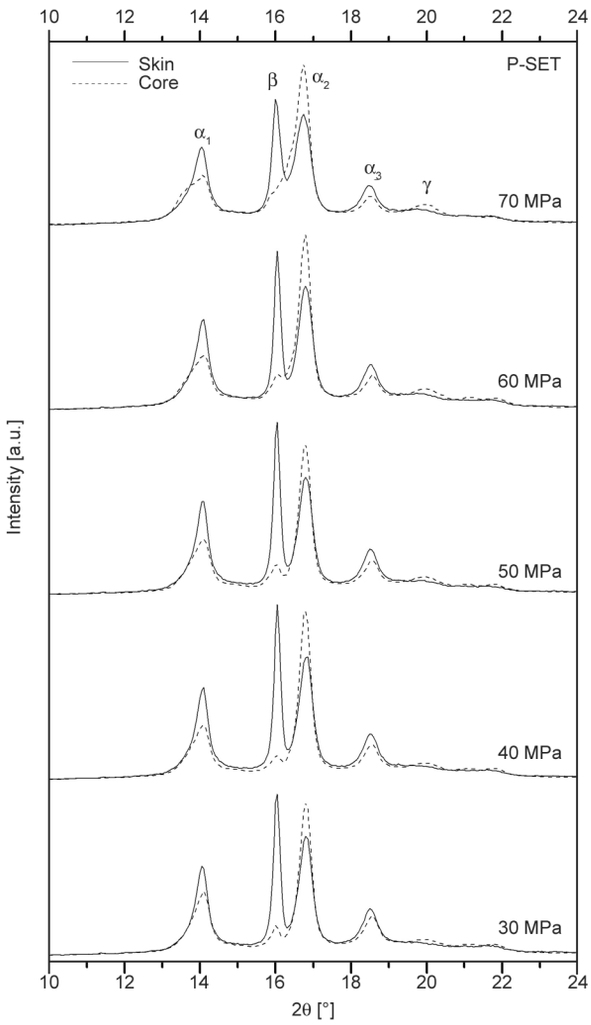

Figure 2. X-ray diffraction patterns of specimens injection-molded with various holding pressures – P-SET.

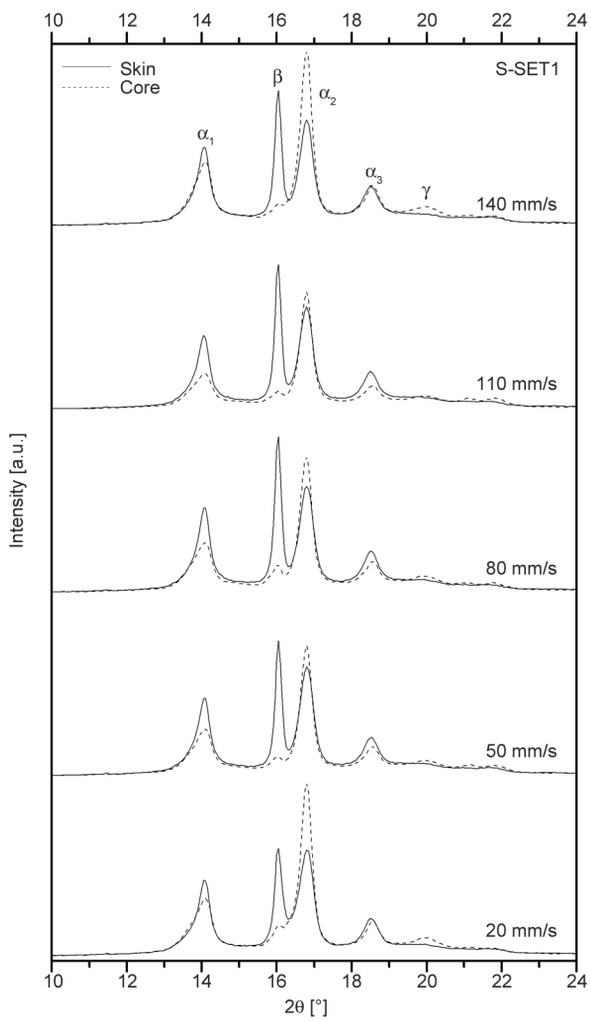

Figure 3. X-ray diffraction patterns of specimens injection-molded in various injection speeds into the mold with the temperature of 40 °C – S-SET1.

are formed due to the presence of stereo- and regio-defects [41], whereas the formation of β-crystals is induced under the flow field. The shearing of polypropylene melt causes the creation of α-row nuclei, which subsequently leads to the growth of the β-phase on the formed α-nuclei [1, 42].

The influence of mold temperature on the content of β- and γ-phases can be seen in Figure 6. The data also indicate that the polymorphic composition of LCB-PP is significantly affected by the skin-core structure. An increase in both phases with increasing mold temperature can be observed, particularly in the case of the γ-phase. Its content in the skin layer doubled from 7 to 14%, while in the core, it increased by about half, from 25 to 37%, for mold temperatures in the range of 40–120 °C which is expected trend based on earlier works [24, 25]. Crystallization temperatures above 110 °C result in nearly exclusive formation of the γ-modification, which is thermodynamically favored over the α-modification [43, 44].

In the case of the β-phase, a slightly higher content of over 40% was observed in the skin layer, and only a small increase in this trigonal phase was observed with increasing mold temperature. However, the formation of the β-phase in the core of LCB-PP was minimally influenced by processing conditions, as its content in all specimens was very low or negligible. The growth rate of the β-modification reaches its maximum at approximately 120 °C [16]. It is known that shear flow leads to oriented or even stretched polymer chains, which subsequently crystallize with different kinetics than under steady-state conditions. The shear flow influences both the nucleation and crystal growth steps. Nevertheless, the flow-enhanced crystallization rate is mainly due to a considerable increase in the nucleation rate and the density of nuclei. In this context, temperature is very crucial because it impacts the relaxation of the polymer chains or their segments. The influence of flow

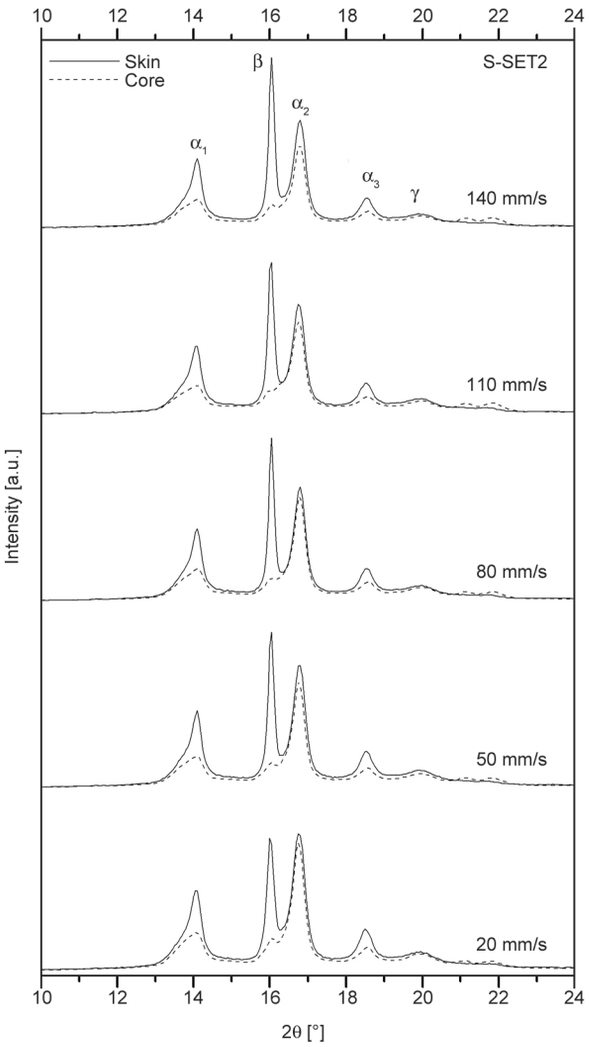

Figure 4. X-ray diffraction patterns of specimens injection-molded in various injection speeds into the mold with the temperature of 120 °C – S-SET2.

on polypropylene nucleation is more effective at high crystallization temperatures because the rate of resting crystallization tends to zero with increasing temperature as the temperature gets near the thermodynamic melting point. However, the orientation

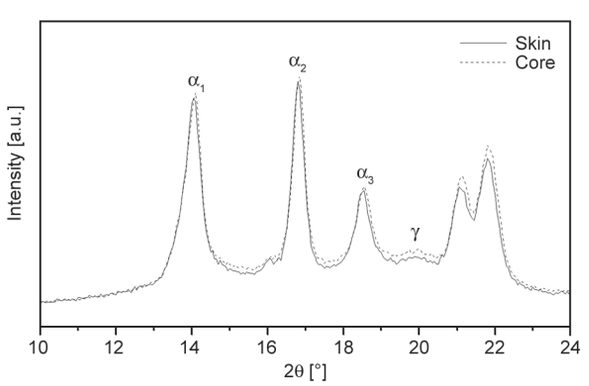

Figure 5. X-ray diffraction patterns of compression-molded specimens.

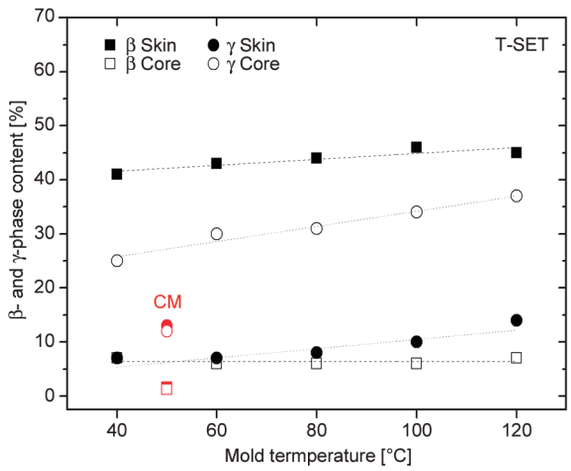

Figure 6. Dependence of β- and γ-phases content on the mold temperature during injection molding – T-SET and compression molding.

induced by flow at this temperature remains [45]. According to Janeschitz-Kriegl and coworkers [46, 47], there is a great amount of poorly organized aggregates of molecular chains that can form efficient nuclei only at quite low temperatures in a steady-state melt. But, the flow can support their growth. Thus, a great number of poor-quality sleeping nuclei are changed into better-quality nuclei, active at high temperatures in shear. Consequently, as the degree of supercooling decreases, the effect of flow on crystallization kinetics becomes more pronounced.

Figure 7 shows the changes in β- and γ-phase content as a function of holding pressure. An increase in holding pressure, from 30 to 70 MPa, results in a significant increase in the orthorhombic γ-phase, particularly in the core, where the growth is approximately 20% (from 17 to 37%). This positive effect of increasing

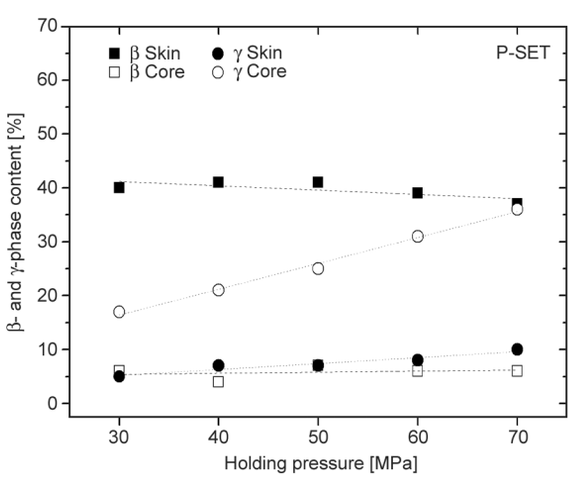

Figure 7. Dependence of β- and γ-phases content on the holding pressure – P-SET.

Table 2. The crystallinity of the specimens *vs*. mold temperature (T-SET), holding pressure (P-SET), injection speed (S-SET1, S-SET2), and compression molding (CM).

T-SET [°C]	Crystallinity [%]		P-SET [MPa]	Crystallinity [%]		S-SET1 [mm/s]	Crystallinity [%]		S-SET2 [mm/s]	Crystallinity [%]	
	Skin	Core		Skin	Core		Skin	Core		Skin	Core
40	70	67	20	69	66	20	70	71	30	72	68
60	70	68	50	66	67	50	69	65	40	71	67
80	71	68	80	70	67	80	70	67	50	71	67
100	71	66	110	67	65	110	69	66	60	70	65
120	71	67	140	66	65	140	67	69	70	72	64
CM	55	54									

pressure on γ-phase formation has also been observed by Navratilova *et al.* [26]. However, the effect of holding pressure within the range of 30–70 MPa on trigonal β-phase content is insignificant, with only a small decrease observed in the skin layer. This decrease may be attributed to a shortening of the crystallization time, whereby the previously mentioned α-nuclei created during melt flow can relax and result in competitive β-phase growth, which decreases with decreasing holding pressure [37].

Interesting results can also be observed in the case of specimens injection-molded at various injection speeds into molds tempered at 40 °C (Figure 8) and 120 °C (Figure 9). The highest increase in the trigonal β-phase content depending on injection speed and mold temperature can be observed in the skin layer. At low injection speeds (20 mm/s), the β-phase content reached 34% independent of mold temperature. As the injection speed increased, the β-phase content also increased, reaching up to 42% at 40 °C mold temperature and even up to 46% at 120 °C. These results are supported by the fact that the enhanced entanglement introduced by LCB prolongs the relaxation time of molecules after deformation. Hence, they can easily initiate the oriented core under shear flow and then give nucleation sites for β-crystal growth. The loosely coiled linear chains can be incorporated on the surface by the orientation of the induced nuclei and crystallize into a β-crystal [4, 37]. A higher mold temperature of 120 °C promoted β-phase formation up to 46% in the skin layer, while the content of β-phase in the core remains relatively low and independent of injection speed, with values of around 5 or 8% at mold temperatures of 40 and 120 °C, respectively. The formation of the orthorhombic γ-phase in the injection-molded specimens was not found to be significantly affected by the injection speed. However, the content of γ-phase was observed to increase with higher crystallization temperatures, reaching 15% in the skin and 35% in the core layer, as compared to 7 and 25%, respectively, at lower temperatures.

3.2. Charpy impact strength

The polymorphic composition of the individual specimens is reflected in their mechanical properties.

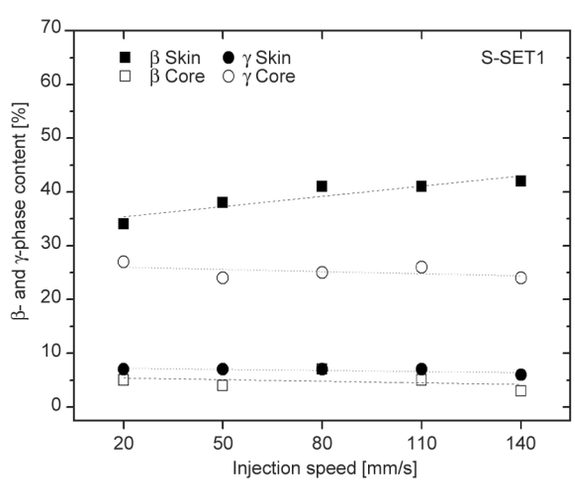

Figure 8. Dependence of β- and γ-phases content on the injection speed into the mold with the temperature of 40 °C – S-SET1.

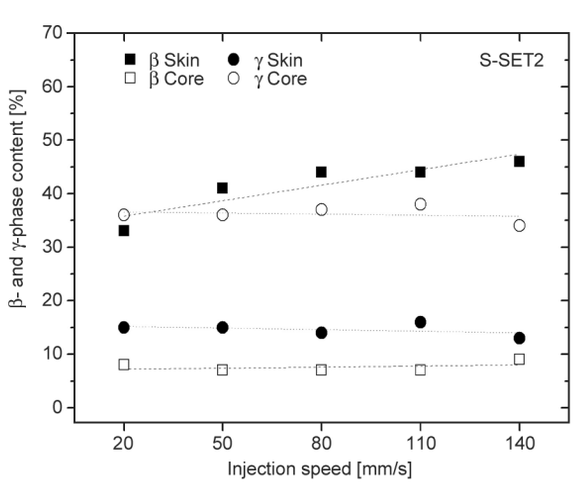

Figure 9. Dependence of β- and γ- phases content on the injection speed into the mold with the temperature of 120 °C – S-SET2.

The occurrence of the trigonal β-phase to a greater extent in the structure of polypropylene leads to a change in impact strength [19]. The impact performance of all specimens – injection-molded in various conditions and compression-molded is summarized in Figure 10. Compression-molded ones reach Charpy impact strength of 4.2 kJ/m^2. In the case of injection-molded specimens positive joint effect of mold temperature and injection speed on impact strength is evident. Increasing injection speed (from 20 to 140 mm/s) at 40 °C of mold temperature leads to an increase in impact strength of about 15% (from 3.8 to 4.4 kJ/m^2). At the same time, it is possible to observe a one-third increase in impact strength at all injection speeds with higher mold temperature (120 °C) – an increase in impact strength from 3.8 kJ/m^2 (mold temperature 40 °C) to 5.1 kJ/m^2 (120 °C) at 20 mm/s speed. Thus, the highest impact strength has been achieved in the specimens injection-molded at a speed of 140 mm/s at the mold temperature of 120 °C, which shows an impact strength of 5.7 kJ/m^2. The effect of holding pressure on the impact strength of the specimens has also been demonstrated – with increasing holding pressure from 30 to 70 MPa, the impact strength increased by 23% from 3.6 to 4.4 kJ/m^2.

Comparison of the results of polymorphic composition (Figures 6–9) and Charpy impact strength (Figure 10) clearly shows that impact strength is positively influenced by β-phase and simultaneously γ-phase content.

4. Conclusions

In the present paper, the impact of processing parameters, including mold temperature, injection speed, and holding pressure, on the supermolecular structure of long-chain branched polypropylene, as well as its impact strength, was investigated. Findings, based on data obtained through wide-angle X-ray scattering, demonstrated that injection speed, mold temperature, and holding pressure all have a significant impact on the polymorphic composition of LCB-PP specimens. Specifically, the joint effect of high injection speed and mold temperature led to the formation of trigonal β-phase in the skin layer. It was found that under shear flow, an oriented center can easily initiate, providing nucleation sites for β-crystal growth. Furthermore, prolonged relaxation times of LCBs after deformation contribute to the incorporation of loosely coined linear chains on the surface, which then orient the induced nuclei and crystallize into β-crystals. In contrast, it was found that growing holding pressure had a significant effect on the γ-phase, primarily in the core of the specimens. The higher content of γ-phase was promoted by higher mold temperature and holding pressure. The results also demonstrated that the polymorphic composition of the individual specimens was reflected in their impact strength. Interestingly, it was found that the co-existence of both β-phase and γ-phase had a favorable impact on the enhancement of impact strength. Overall, this study sheds new light on the importance of processing parameters in controlling

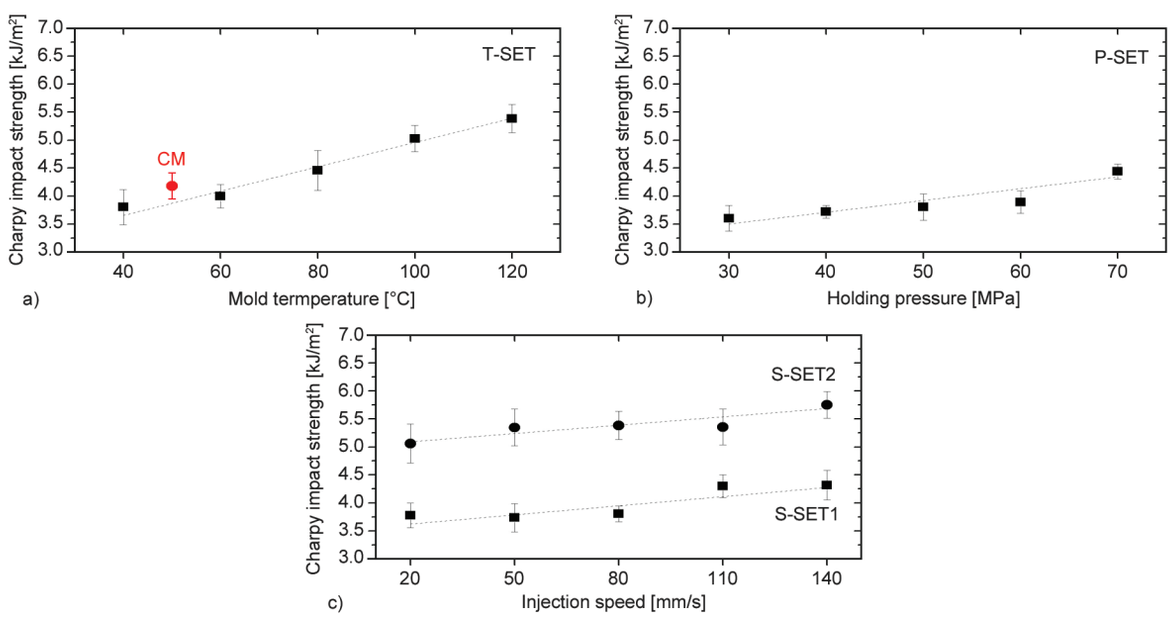

Figure 10. Variations of the Charpy impact strength for specimens processed at various conditions: a) T-SET and compression-molded (CM), b) P-SET, c) S-SET1 and S-SET2.

the supermolecular structure and impact strength of LCB-PP, which could have significant implications in the design and manufacture of polymeric materials.

References

[1] Somani R. H., Hsiao B. S., Nogales A., Fruitwala H., Srinivas S., Tsou A. H.: Structure development during shear flow induced crystallization of i-PP: *In situ* wide-angle X-ray diffraction study. Macromolecules, **34**, 5902–5909 (2001). https://doi.org/10.1021/ma0106191

[2] Kalay G., Bevis M. J.: Processing and physical property relationships in injection-molded isotactic polypropylene. 2. Morphology and crystallinity. Journal of Polymer Science Part B: Polymer Pysics, **35**, 265–291 (1997). https://doi.org/10.1002/(SICI)1099-0488(19970130)35:2<265::AID-POLB6>3.0.CO;2-R

[3] Varga J.: Supermolecular structure of isotactic polypropylene. Journal of Material Science, **27**, 2557–2579 (1992). https://doi.org/10.1007/BF00540671

[4] Sun H., Zhao Z., Yang Q., Yang L., Wu P.: The morphological evolution and β-crystal distribution of isotactic polypropylene with the assistance of a long chain branched structure at micro-injection molding condition. Journal of Polymer Research, **24**, 75 (2017). https://doi.org/10.1007/s10965-017-1234-3

[5] Huo H., Jiang S., An L., Feng J.: Influence of shear on crystallization behavior of the β phase in isotactic polypropylene with β-nucleating agent. Macromolecules, **37**, 2478–2483 (2004). https://doi.org/10.1021/ma0358531

[6] Zuo F., Keum J. K., Yang L., Somani R. H., Hsiao B. S.: Thermal stability of shear-induced shish-kebab precursor structure from high molecular weight polyethylene chains. Macromolecules, **39**, 2209–2218 (2006). https://doi.org/10.1021/ma052340g

[7] Zhang B., Chen J., Cui J., Zhang H., Ji F., Zheng G., Heck B., Reiter G., Shen C.: Effect of shear stress on crystallization of isotactic polypropylene from a structured melt. Macromolecules, **45**, 8933–8937 (2012). https://doi.org/10.1021/ma3014756

[8] Gahleitner M., Mileva D., Androsch R., Gloger D., Tranchida D., Sandholzer M., Doshev P.: Crystallinity-based product design: Utilizing the polymorphism of isotactic PP homo- and copolymers. International Polymer Processing, **31**, 618–627 (2016). https://doi.org/10.3139/217.3242

[9] Lotz B. A.: A new ε crystal modification found in stereodefective isotactic polypropylene samples. Macromolecules, **47**, 7612–7624 (2014). https://doi.org/10.1021/ma5009868

[10] Rieger B., Mu X., Mallin D. T., Chien J. C. W., Rausch M. D.: Degree of stereochemical control of racemic ethylenebis(indenyl)zirconium dichloride/methyl aluminoxane catalyst and properties of anisotactic polypropylenes. Macromolecules, **23**, 3559–3568 (1990). https://doi.org/10.1021/ma00217a005

[11] Chvátalová L., Navrátilová J., Čermák R., Raab M., Obadal M.: Joint effects of molecular structure and processing history on specific nucleation of isotactic polypropylene. Macromolecules, **42**, 7413–7417 (2009). https://doi.org/10.1021/ma9005878

[12] Lovinger A. J., Chua J. O., Gryte C. C.: Studies on the α and β forms of isotactic polypropylene by crystallization in a temperature gradient. Journal of Polymer Science: Polymer Physics Edition, **15**, 641 (1977). https://doi.org/10.1002/pol.1977.180150405

[13] Karger-Kocsis J., Varga J.: Effects of β-α transformation on the static and dynamic tensile behavior of isotactic polypropylene. Journal of Applied Polymer Science, **62**, 291–300 (1996). https://doi.org/10.1002/(SICI)1097-4628(19961010)62:2<291::AID-APP4>3.0.CO;2-S

[14] Somani R. H., Hsiao B. S., Nogales A., Srinivas S., Tsou A. H., Sics I., Balta-Calleja F. J., Ezquerra T. A.: Structure development during shear flow-induced crystallization of i-PP: *In-situ* small-angle X-ray scattering study. Macromolecules, **33**, 9385–9394 (2000). https://doi.org/10.1021/ma001124z

[15] Gajzlerova L., Navratilova J., Ryzi A., Slabenakova T., Cermak R.: Joint effects of long-chain branching and specific nucleation on morphology and thermal properties of polypropylene blends. Express Polymer Letters, **14**, 952–961 (2020). https://doi.org/10.3144/expresspolymlett.2020.77

[16] Varga J.: β-modification of isotactic polypropylene: Preparation, structure, processing, properties, and application. Journal of Macromolecular Science Part B, **41**, 1121–1171 (2002). https://doi.org/10.1081/MB-120013089

[17] Romankiewicz A., Sterzynski T., Brostow W.: Structural characterization of α- and β-nucleated isotactic polypropylene. Polymer International, **53**, 2086–2091 (2004). https://doi.org/10.1002/pi.1632

[18] Grein C.: Toughness of neat, rubber modified and filled β-nucleated polypropylene: From fundamentals to applications. in 'Intrinsic molecular mobility and toughness of polymers II' (ed.: Kausch H. H.) Vol. 188, 43–104 (2005). https://doi.org/10.1007/b136972

[19] Obadal M., Čermák R., Baran N., Stoklasa K., Simonik J.: Impact strength of β-nucleated polypropylene. International Polymer Processing, **19**, 35–39 (2004). https://doi.org/10.3139/217.1802

[20] Čermák R., Obadal M., Ponížil P., Polášková M., Stoklasa K., Lengálová A.: Injection-moulded α- and β-polypropylenes: I. Structure *vs*. processing parameters. European Polymer Journal, **41**, 1838–1845 (2005). https://doi.org/10.1016/j.eurpolymj.2005.02.020

[21] Navrátilová J., Čermák R., Obadal M., Verney V., Commereuc S.: Effect of β-nucleation on crystallization of photodegraded polypropylene. Journal of Thermal Analysis and Calorimetry, **95**, 215–220 (2009). https://doi.org/10.1007/s10973-008-8892-7

[22] Výchopňová J., Čermák R., Obadal M., Raab M., Verney V., Commereuc S.: The role of specific nucleation in polypropylene photodegradation. Polymer Degradation and Stability, **92**, 1763–1768 (2007). https://doi.org/10.1016/j.polymdegradstab.2007.07.010

[23] Obadal M., Čermák R., Raab M., Verney V., Commereuc S., Fraïsse F.: Study on photodegradation of injection-moulded β-polypropylenes. Polymer Degradation and Stability, **91**, 459–463 (2006). https://doi.org/10.1016/j.polymdegradstab.2005.01.046

[24] Thomann R., Wang C., Kressler J., Mülhaupt R.: On the γ-phase of isotactic polypropylene. Macromolecules, **29**, 8425–8434 (1996). https://doi.org/10.1021/ma951885f

[25] Hosier I. L., Alamo R. G., Esteso P., Isasi J. R., Mandelkern L.: Formation of the α and γ polymorphs in random metallocene–propylene copolymers. Effect of concentration and type of comonomer. Macromolecules, **36**, 5623–5636 (2003). https://doi.org/10.1021/ma030157m

[26] Navratilova J., Gajzlerova L., Kovar L., Cermak R.: Long-chain branched polypropylene: Crystallization under high pressure and polymorphic composition. Journal of Thermal Analysis and Calorimetry, **143**, 3377–3383 (2021). https://doi.org/10.1007/s10973-020-09931-1

[27] Morrow D. R., Newman B. A.: Crystallization of low-molecular-weight polypropylene fractions. Journal of Applied Physics, **39**, 4944–4950 (1968). https://doi.org/10.1063/1.1655891

[28] Hosier I. L., Alamo R. G., Lin J. S.: Lamellar morphology of random metallocene propylene copolymers studied by atomic force microscopy. Polymer, **45**, 3441–3455 (2004). https://doi.org/10.1016/j.polymer.2004.02.071

[29] Langston J. A., Colby R. H., Chung T. C. M., Shimizu F., Suzuki T., Aoki M.: Synthesis and characterization of long chain branched isotactic polypropylene *via* metallocene catalyst and T-reagent. Macromolecules, **40**, 2712–2720 (2007). https://doi.org/10.1021/ma062111+

[30] Zhang X., Wang X., Huang J., Xia Z.: Quasi-static and dynamic piezoelectric d_{33} coefficients of irradiation cross-linked polypropylene ferroelectrets. Journal of Materials Science, **44**, 2459–2465 (2009). https://doi.org/10.1007/s10853-009-3312-3

[31] Zhang Z. J., Wan D., Xing H. P., Zhang Z. J., Tan H. Y., Wang L., Zheng J., An Y. J. Tang T.: A new grafting monomer for synthesizing long chain branched polypropylene through melt radical reaction. Polymer, **53**, 121–129 (2012). https://doi.org/10.1016/j.polymer.2011.11.033

[32] Wang K., Wang S., Wu F., Pang Y., Liu W., Zhai W., Zheng W.: A new strategy for preparation of long-chain branched polypropylene *via* reactive extrusion with supercritical CO_2 designed for an improved foaming approach. Journal of Materials Science, **51**, 2705–2715 (2016). https://doi.org/10.1007/s10853-015-9584-x

[33] Su Z., Wang H., Dong J., Zhang X., Dong X., Zhao Y., Yu J., Han C. C., Xu D., Wang D.: Conformation transition and crystalline phase variation of long chain branched isotactic polypropylenes (LCB-iPP). Polymer, **48**, 870–876 (2007). https://doi.org/10.1016/j.polymer.2006.12.013

[34] Tian J., Yu W., Zhou C.: Crystallization behaviors of linear and long chain branched polypropylene. Journal of Applied Polymer Science, **104**, 3592–3600 (2007). https://doi.org/10.1002/app.26024

[35] McCallum T. J., Kontopoulou M., Park C. B., Muliawan E. B., Hatzikiriakos S. G.: The rheological and physical properties of linear and branched polypropylene blends. Polymer Engineering and Science, **47**, 1133–1140 (2007). https://doi.org/10.1002/pen.20798

[36] Nam G. J., Yoo J. H., Lee J. W.: Effect of long-chain branches of polypropylene on rheological properties and foam-extrusion performances. Journal of Applied Polymer Science, **96**, 1793–1800 (2005). https://doi.org/10.1002/app.21619

[37] Zhou S., Wang W., Xin Z., Zhao S., Shi Y.: Relationship between molecular structure, crystallization behavior, and mechanical properties of long chain branching polypropylene. Journal of Materials Science, **51**, 5598–5608 (2016). https://doi.org/10.1007/s10853-016-9856-0

[38] Wang L., Ishihara S., Ando M., Minato A., Hikima Y., Ohshima M.: Fabrication of high expansion microcellular injection-molded polypropylene foams by adding long-chain branches. Industrial and Engineering Chemistry Research, **55**, 11970–11982 (2016). https://doi.org/10.1021/acs.iecr.6b03641

[39] Obadal M., Čermák R., Stoklasa K: Tailoring of three-phase crystalline systems in isotactic poly(propylene). Macromolecular Rapid Communications, **26**, 1253–1257 (2005). https://doi.org/10.1002/marc.200500272

[40] Turner-Jones A., Aizlewood J. M., Beckett D. R.: Crystalline forms of isotactic polypropylene. Macromolecular Chemistry and Physics, **75**, 134–158 (1964). https://doi.org/10.1002/macp.1964.020750113

[41] Sauer J. A., Pae K. D.: Structure and thermal behavior of pressure-crystallized polypropylene. Journal of Applied Physics, **39**, 4959–968 (1968). https://doi.org/10.1063/1.1655893

[42] Varga J., Karger-Kocsis J.: Rules of supermolecular structure formation in sheared isotactic polypropylene melts. Journal of Polymer Science Part B: Polymer Physics, **34**, 657–670 (1996). https://doi.org/10.1002/(SICI)1099-0488(199603)34:4<657::AID-POLB6>3.0.CO;2-N

[43] Zhao W., Huang Y., Liao X., Yang Q.: The molecular structure characteristics of long chain branched polypropylene and its effects on non-isothermal crystallization and mechanical properties. Polymer, **54**, 1455–1462 (2013). https://doi.org/10.1016/j.polymer.2012.12.073

[44] Wood-Adams P. M., Dealy J. M., deGroot A. W., Redwine O. D.: Effect of molecular structure on the linear viscoelastic behavior of polyethylene. Macromolecules, **33**, 7489–7499 (2000). https://doi.org/10.1021/ma991533z

[45] Liu Q., Sun X., Li H., Yan S.: Orientation-induced crystallization of isotactic polypropylene. Polymer, **54**, 4404–4421 (2013). https://doi.org/10.1016/j.polymer.2013.04.066

[46] Janeschitz-Kriegl H., Ratajski E., Stadlbauer M.: Flow as an effective promotor of nucleation in polymer melts: A quantitative evaluation. Rheologica Acta, **42**, 355–364 (2003). https://doi.org/10.1007/s00397-002-0247-x

[47] Janeschitz-Kriegl H.: A recollection with respect to flow induced crystallization in polymer melt processing. International Polymer Processing, **32**, 227–236 (2017). https://doi.org/10.3139/217.3331